GSC 4552-1498: A new triple-mode high-amplitude δ Scuti star discovered by *TESS*

Xiao-Ya Sun[1], Zhao-Yu Zuo[1], Tao-Zhi Yang[1]

ABSTRACT

In this paper, the pulsation behavior of high-amplitude δ Scuti (HADS) star GSC 4552-1498 was analyzed. Using the high-precision photometric data from *TESS*, two new independent frequencies $F1 = 22.6424(1)$ d^{-1} and $F2 = 28.6803(5)$ d^{-1} were identified for this source, along with the fundamental one $F0 = 17.9176(7)$ d^{-1}, which was previously known. The period ratios of $F0/F1 = 0.791$ and $F0/F2 = 0.625$ reveal that $F1$ and $F2$ are the first and second overtone radial modes, respectively. Therefore GSC 4552-1498 was reclassified as a radial triple-mode HADS star in this study, rather than single-mode as once thought. In addition, the classical $O-C$ analysis was conducted, by combining 79 times of maximum light previously known with 1351 newly determined ones in this work, to give a new ephemeris formula of $BJD_{max} = T_0 + P \times E$ = 2453321.534728(1) + 0.055811(0) $\times$ E. The $O-C$ diagram reveals a continuous period increase, but the rate of $(1/P)(dP/dt) = 9.54(8) \times 10^{-8}$ yr^{-1} seems much larger (~ 100) than predicted by evolution theories. We note this discrepancy has long been established, but not well explained, possibly related to nonlinear mode interaction but still need further investigation. Based on frequency parameters (i.e., $F0$, $F1$ and $F2$), a series of theoretical models were conducted by employing the stellar evolution code. Due to the degeneracy between mass and metallicity, the stellar parameters of GSC 4552-1498 can only be simply constrained as: mass $M = 1.14^{+0.16}_{-0.01}$ M$_\odot$, $Z = 0.006^{+0.006}_{-0.000}$, $T_{eff} = 6598^{+36}_{-40}$ K and $\log(L/L_\odot) = 0.5735^{+0.0407}_{-0.0121}$. We note GSC 4552-1498 is located on the main-sequence (MS) in the H-R diagram.

Subject headings: stars: individual (GSC 4552-1498) - stars: oscillations - stars: variable: delta Scuti

1. Introduction

One of the long-standing goals in astronomy is to improve our understanding of stellar evolution by constraining the unknown interior physics of stars. At present, the only method to detect

[1] Ministry of Education Key Laboratory for Nonequilibrium Synthesis and Modulation of Condensed Matter, School of physics, Xi'an Jiaotong University, Xi'an 710049, People's Republic of China; zuozyu@xjtu.edu.cn

the interior physics of star is astroseismology, which uses the resonant pulsation frequencies of a star to constrain its interior properties from a quantitative comparison to stellar models including different input physics (Aerts 2021). The high-precision time series photometric data from space-based telescopes such as *Kepler* (Borucki et al. 2010; Balona & Dziembowski 2011; Uytterhoeven et al. 2011) and *TESS* (Ricker et al. 2015; Antoci et al. 2019) provide us an excellent opportunity to detect the period and amplitude of more pulsation modes besides the fundamental one (Antoci et al. 2019). δ Scuti stars are a class of intermediate-mass stars with periods in range of 0.02-0.25 days and spectral types from A to F. They locate in the classical Cepheid instability strip across the main sequence (MS) in the H-R diagram and exhibit both radial and nonradial pulsation modes (Breger 2000; Qian et al. 2018). These characteristics make them excellent sources for astroseismology study.

High-amplitude δ Sct (HADS) stars are a subclass of δ Sct stars with peak-to-peak light amplitudes larger than 0.3 mag. They are traditionally found to be slow rotators with $\nu \sin i < 30$ km s^{-1} and pulsation periods between 1 and 6 h (McNamara 2000). From the ground-based observations, HADS stars typically have only one or two radial pulsation modes, in the fundamental and/or first overtone mode (Balona et al. 2012). According to Lee et al. (2008), the HADS stars are rare, which is estimated to account for only 0.3 % of all the Galactic population of δ Sct stars. Moreover, during the *Kepler* mission, more than 10000 A and F stars were found, of which only two HADS stars (Balona 2016; Bowman 2016; Bowman et al. 2021). And most HADS stars are single-mode, a small part double-mode, while very few are triple-mode. In addition, the AAVSO International Variable Star Index (VSX; Watson et al. 2015) lists about 600 HADS stars, of which 85 double-mode HADS stars, however, only five triple-mode HADS stars identified and studied in detail, i.e., AC And (Fitch & Szeidl 1976), V829 AqI (Handler et al. 1998), V823 (Jurcsik et al. 2006), GSC 762-110 (Wils et al. 2008) and GSC 03144-595 (Mow et al. 2016). The sample of triple-mode HADS star seems still largely lacking.

In recent decades, thanks to the high photometric precision observations from space telescopes such as *Kepler* and *TESS*, several HADS stars have been discovered to have non-radial modes, not only the radial modes (Poretti et al. 2011). And several show interesting features, such as the amplitude modulation and low-amplitude pulsation modes. For example, Yang et al. (2018b) detected a weak modulation effect around the dominant pulsation modes in KIC 5950759, and suggested that the reason might be due to the amplitude modulation of the radial modes from stellar rotation. Subsequently, Bowman et al. (2021) revealed that KIC 5950759 has not only two dominant radial pulsation modes, but also non-radial pulsation modes. Moreover, the HADS star KIC 10284901 shows a quintuplet structure in the frequency spectra, which might be related to the Blazhko effect (Yang & Esamdin 2019). We note there is one more triple-mode HADS candidate recently discovered (i.e., KIC 10975348; Yang et al. 2021) by using the *Kepler* data, due to the identification of a low-amplitude frequency in this star. Based on the high-precision time series

photometric data from *TESS*, more pulsation modes (i.e., triple- even multi-mode) are expected to be detected, which provide an opportunity for us to improve our knowledge of HADS stars.

GSC 4552-1498 (α_{2000}=$11^h24^m25^s.350$, δ_{2000}=+$77^\circ42'15''.629$, 2MASS: J11242535+7742156), was discovered by A.V. Khruslovas, who classified the star as an HADS with a pulsation period of 0.05581096 days. Its amplitude changed from 12.9 to 13.4 mag (Jafarzadeh & Poro 2017). Jafarzadeh & Poro (2017) derived the frequencies of the fundamental mode $F0$ = 17.899 d^{-1} and its harmonic $2F0$ = 35.204 d^{-1} from the ground-based observations. According to the empirical relations, they calculated several parameters of GSC 4552-1498: the effective temperature T_{eff} = 7766 ($\pm$ 59) K, luminosity L = 9.09 ($\pm$ 2.50) $L_\odot$, mass M = 1.68 ($\pm$ 0.10) $M_\odot$ and radius is 1.67 $R_\odot$. They also obtained 4 times of maximum light in 2017. During 2009 and 2014, 75 more maxima were collected by Wils et al. (2009, 2012, 2013, 2014, 2015). Some basic parameters of GSC 4552-1498 are listed in Table 1. In order to limit the parameters more accurately and investigate its long-term periodic variation, we downloaded the high-precision photometric data provided by *TESS* and conducted a detailed study.

2. OBSERVATIONS AND DATA REDUCTION

GSC 4552-1498 was observed by *TESS* (Ricker et al. 2015) during Sectors 14, 20 and 21, from BJD 2458683.346 to 2458897.782 in 2 min cadence. All the data were downloaded from *TESS* Asteroseismic Science Operations Center (TASOC) database[1]. In this work, we converted the corrected flux to stellar magnitudes and performed corrections, including eliminating the outliers and detrending the light curve. Then the mean value of each sector was subtracted, and the rectified time series was obtained with 53568 data points in total, spanning over about 214 days. A section of the rectified light curves of GSC 4552-1498 was shown in Figure 1. The light curve shows a faster rise than the decline with a peak-to-peak amplitude of about 0.4 mag, which is typical for HADS stars (McNamara 2000).

3. FREQUENCY ANALYSIS

In this work, the *TESS* data of GSC 4552-1498 were searched for significant frequencies using PERIOD04 (Lenz & Breger 2005), which was based on the Fourier transformations. The light curve was fitted with the following formula:

[1]TASOC database: https://tasoc.dk

$$m = m_0 + \Sigma A_i sin(2\pi(f_i t + \phi_i)), \quad (1)$$

where m_0 is the zero-point, A_i is the amplitude, f_i is the frequency, and ϕ_i is the corresponding phase.

To detect more significant frequencies, we chose a frequency range of $0 < \nu < 100$ d^{-1}, which covers the pulsation frequency of δ Scuti stars. At each step in the process of extracting frequency, the frequency of the highest amplitude peak was determined as a significant frequency, then optimized to the light curve using formula (1), and the solutions of frequency and amplitude were obtained. Then the light curve constructed using the above solutions was subtracted from the data, and the residual was used as input in the next step. The above steps were repeated until there was no significant peak in the residual. The standard stop criterion of a signal-to-noise (S/N) > 4.0 (Breger et al. 1993) was chosen to extract all significant frequencies. The uncertainties of all frequencies were calculated following the method provided by Montgomery & Odonoghue (1999).

The initial amplitude spectra was shown in the top panel of Figure 2, in which the frequency of the highest amplitude peak (F0) was labelled. We removed F0 to produce the amplitude spectra in the second panel, where the four harmonic frequencies of F0 were visible. The last panel shows the amplitude spectra of the residuals after 13 detected frequencies were removed from the data. Following Breger et al. (1993), we drew the detection limit at a signal-to-noise (S/N) = 4.0 for the judgment of a significant peak. There is no obvious peak in the residuals and the overall distribution of the residual is typical noise.

The solutions of 13 frequencies with S/N > 4.0 are listed in Table 2, including 2 frequencies which are consistent with those found by Jafarzadeh & Poro (2017) and 11 frequencies newly detected in this work. The frequency of the highest amplitude was usually assumed to be the fundamental radial mode, since the light variations were dominated by this frequency. Therefore, we marked f_{S1} as F0 in Table 2. The period ratio of $P_1/P_0 = f_{S1}/f_{S8} = 0.791$, which is close to the result (0.756-0.787) from Petersen & Christensen-Dalsgaard (1996), indicates that f_{S8} is the first overtone. And f_{S1} and f_{S6} have a period ratio of 0.625 (0.611-0.632) identifying f_{S6} as the second overtone radial mode (Breger 2000; Petersen & Christensen-Dalsgaard 1996; Stellingwerf 1979). Therefore, we marked f_{S8} and f_{S6} as F1 and F2, respectively. We note these two independent frequencies were firstly identified in this study. Due to this discovery, the source GSC 4552-1498 was reclassified as a radial triple-mode HADS star, instead of single-mode as previously thought. Another similar sample is KIC 10975348 (Yang et al. 2021), in which a low-amplitude frequency was detected recently, by using the *Kepler* data. It is very encouraging that in the space era, more sources with much weaker pulsation modes could be detected, while it might be missed (i.e., fall in the noise) in the ground-based era. Since mode identification is of great importance in seismic modelings, hence the study of stellar structure and evolution. We urge that a larger such sample is

still needed in near future.

4. $O-C$ Diagram

We used the $O-C$ technique to detect the long-term period changes of GSC 4552-1498. $O-C$ is the difference between the observed and calculated maximum times (Sterken 2005). The observed times of maximum light were determined by fitting the light curves. We made a second-order polynomial fit to a part of the light curves around each maximum. Generally, we chose a range with an amplitude of around one-third of the full amplitude, since this section of the light curves can reach a satisfactory fit. The fitting errors typically 0.00001 d^{-1} were estimated using Monte Carlo simulations (Lenz & Breger 2005). Finally, 1351 new maximum times were obtained from the *TESS* data and listed in Table A1 in the Appendix.

In order to make $O-C$ analysis of GSC 4552-1498, the newly determined times of maximum light were considered together with those provided by earlier studies: the maxima with numbers 19, 13, 20, 7, 16 and 4 obtained by Wils et al. (2009, 2012, 2013, 2014, 2015) and Jafarzadeh & Poro (2017), respectively. Then, these times of maximum light from ground-based observations (total: 79, summarized in Table A2 in the Appendix), which were originally in HJD, were converted to BJD to be consistent in both time-scale and format with the *TESS* data.

A total of 1430 maxima were collected. To obtain the calculated times of maximum light, $O-C$ values and their corresponding cycles, we fitted the 1430 maximum times with a straight-line and derived a new ephemeris formula:

$$BJD_{max} = T_0 + P \times E = 2453321.534728(1) + 0.055811(0) \times E, \quad (2)$$

where T_0, P and E is the initial epoch, period and the cycle number, respectively. And this ephemeris formula is consistent with the linear ephemeris given by Jafarzadeh & Poro (2017): T = 2453321.53540 + 0.05581097 $\times$ E. All the $O-C$ values and the corresponding cycle numbers were listed in Table A1 and Table A2 in the Appendix, respectively. The $O-C$ diagram was shown in Figure 3, where the blue dots represent the previous 79 points and the red dots are the 1351 new points.

We made a second-order polynomial fit to the 1430 points. The new ephemeris was obtained:

$$BJD_{max} = 2453321.535854(1) + 0.055811(0) \times E + 4.07(9) \times 10^{-13} \times E^2, \quad (3)$$

with the standard deviation of the fitting residuals of 0.00029 day.

In the lower instability strip where the δ Scuti stars are found, stellar evolution theory predicts an increasing period in most of stars (Breger & Pamyatnykh 1998). And in pulsating stars, when a pulsation period changes linearly with time, the $O-C$ diagram will show a parabolic form that rises or falls depending on whether the period is increasing or decreasing (Sterken 2005). For GSC 4552-1498, from the $O-C$ diagram in Figure 3, the parabolic fit reveals a continuously increasing period change. From the equation (3), the quadratic term indicates the rate of period change $(1/P)(dP/dt) = 9.54(8) \times 10^{-8}\ yr^{-1}$.

5. Stellar Models and Fitting Results

In order to obtain more precise mass and evolutionary stage of GSC 4552-1498, we used the Modules for Experiments in Stellar Astrophysics (*MESA*; Paxton et al. 2011, 2013, 2015, 2018, 2019) to construct the theoretical models. In particular, the 1D stellar evolution module *MESA* star combines a large of numerical and physical modules for simulations of many of stellar evolution. At each step along with the evolutionary tracks, the stellar oscillation code GYRE (Townsend & Teitler 2013) was used to calculate the pulsation frequencies for each specific model. In addition, *MESA* uses the standard mixing-length theory (MLT) of convection provided by Cox & Giuli (1968) and the modified MLT of Henyey et al. (1965).

The evolution and interior structure of a star mainly depend on the initial mass and chemical ingredient. In this work, the stellar mass M was adopted between 1.1 $M_\odot$ and 2.7 $M_\odot$ in steps of 0.01 $M_\odot$, which cover the typical mass range of HADS stars (McNamara 2000). Due to a lack of reliable value of metallicity Z from spectrum, we considered to survey a range with different metallicity values in the interval from 0.002 to 0.030 dex with a step of 0.002 dex. In addition, we adopted the mixing-length parameter $\alpha_{MLT} = 1.77$, which does not affect the results significantly. The effect of stellar rotation was not included in our calculations since the HADS star usually rotates slowly (McNamara 2000). Each model in the above grid was evolved from the zero-age MS to the post MS stage. The pulsation frequencies were calculated using the GYRE program for every step in the evolutionary tracks.

To find the best-fitting model to the observation, we calculated the values of χ^2 of all models by comparing model frequencies with the observed frequencies $F0$, $F1$, and $F2$, according to the following formula (i.e., Eq. 5, Chen et al. 2019),

$$\chi^2 = \frac{1}{k}\sum(|\nu_{obs,i} - \nu_{mod,i}|^2), \tag{4}$$

where $\nu_{obs,i}$, $\nu_{mod,i}$ and k represent the observed frequencies, the corresponding model calcu-

lated values and the number of observed pulsation modes, respectively. The smaller χ^2 is, the higher the probability of the fitting to the observations would be.

In Figure 4, the probability of the fitting across the mass-metallicity plane was displayed. Each lattice represents the minimum value of χ^2 for each specific model. The bluer means the larger the value of $1/\chi^2$, hence smaller χ^2, which gives a higher probability for the fitting. We note it is clear that there exists a mass-metallicity degeneracy of the fittings (the blue strip in the figure), which is similar to that found by Bowman et al. (2021). Due to this degeneracy, we suggest high-resolution spectra is highly desired in the future, which would help not only give an accurate determination of the metallicity that breaks the degeneracy, but also provide other parameters, such as effective temperature, which could further narrow down the parameter space of the star.

Despite this limitation mentioned above, a preliminary constraints on the stellar parameters could still be determined. We selected several best-fitting models as listed in Table 3, with a threshold of $1/\chi^2 \geq 23$ resulting in eight model candidates. With the minimum value of χ^2 as the best model, the stellar parameters of GSC 4552-1498 were simply constrained as: mass $M = 1.14^{+0.16}_{-0.01}$ $M_\odot$, $Z = 0.006^{+0.006}_{-0.000}$, $T_{eff} = 6598^{+36}_{-40}$ K and $\log(L/L_\odot) = 0.5735^{+0.0407}_{-0.0121}$, as listed in Table 4. We note that the mass of GSC 4552-1498 we obtained is different from that by Jafarzadeh & Poro (2017, i.e., $M = 1.68$ ($\pm$ 0.10) $M_\odot$). They simply used empirical relations, such as period-luminosity relationship, which contains considerable scatter (Ziaali et al. 2019), and ignored the effect of metallicity totally, which we thought may account for this discrepancy.

In addition, we calculated the rate of period change for each best-fitting model in order to compare with observations. The results were listed in Table 3 (the last second column), as well. It is notable that all predicted rates of period change are significantly smaller than the value we obtained from $O-C$, by about two orders of magnitude. We note this discrepancy has long been established for δ Scuti stars (Rodríguez et al. 1995; Breger & Pamyatnykh 1998; Rodríguez & Breger 2001; Bowman et al. 2016, 2021), which may not be accounted for solely by stellar evolution. The possible reason is still uncertain, possibly due to nonlinear mode interaction, resonant mode coupling (Breger & Montgomery 1998) and/or in special cases mass-accretion in binaries (DY Peg, Xue & Niu 2020), all of which still need further investigation. A larger sample of δ Scuti stars with similar temporal properties to GSC 4552-1498 is no doubt helpful to further address this issue.

In Figure 5, we show the evolutionary tracks from the zero-age MS to the post-MS stage for the best-fitting models in order to better understand the evolution of GSC 4552-1498. The color lines represent different combinations of metallicity Z and mass M. The crosses mark the minimum χ^2 for each specific model. And the star symbols mark the terminal-age main sequence (TAMS, with core hydrogen content less than 10^{-3}) for each model. We note all these models suggest that GSC 4552-1498 is located on the MS in the H-R diagram. When compared with another five

HADS stars (see Table 12 in Xue et al. 2018), we note GSC 4552-1498 has the shortest P_0. Using the basic pulsation relation $P\sqrt{\bar{\rho}/\rho_{\odot}}$ = Q (P is the period and Q is the pulsation constant), the mean density $\bar{\rho}$ could be roughly estimated. Then this leads to the largest $\bar{\rho}$ for GSC 4552-1498 among this six HADS, revealing that GSC 4552-1498 is still at an earlier stage than the others. Our result is consistent with the tendency derived by Xue et al. (2018), that the lower the fundamental frequency is, the later the star would have evolved into (also see Figure 9 in Xue et al. 2018).

6. SUMMARY

By analyzing the light variations of GSC 4552-1498 using photometric data delivered from the *TESS* mission, we detected 13 significant frequencies (see Table 2) including three independent frequencies $F0$ = 17.9176 d^{-1}, $F1$ = 22.6424 d^{-1} and $F2$ = 28.6803 d^{-1}. Among them, $F1$ and $F2$ were newly detected in this work and $F0$ is also consistent with previous study (See Table 1, Jafarzadeh & Poro 2017). Based on the ratios of $F0/F1$ and $F1/F2$, GSC 4552-1498 was identified to be a new radial triple-mode HADS star firstly in this study.

We obtained the $O-C$ diagram with 1430 times of maximum light including 1351 from *TESS* mission in this work (see Table A1) and 79 from the literature (see Table A2), and derived a new ephemeris: $BJD_{max} = T_0 + P \times E = 2453321.534728(1) + 0.055811(0) \times E$. In addition, the change of period of GSC 4552-1498 was determined for the first time in this work, i.e., increasing continuously with a rate of $(1/P)(dP/dt) = 9.54(8) \times 10^{-8}\ yr^{-1}$, which is about two orders of magnitude larger than predicted by evolution theories (See Table 3, the last second column). The possible reason might be related to nonlinear mode interaction but still need further investigation.

The stellar evolutionary models were constructed with different mass M and Z using *MESA*. By comparing the observed values of $F0$, $F1$ and $F2$ with models, the stellar parameters of GSC 4552-1498 was preliminarily determined (see Table 4), but still suffered from great uncertainties, mainly caused by mass-metallicity degeneracy (see Figure 4, the blue strip). We suggest high-resolution spectral observation in the future is needed to accurately determine the steller parameters. Consequently, GSC 4552-1498 was identified to be a new radial triple-mode HADS star with a continuously increasing period change, and located on the MS stage in the H-R diagram.

This research is supported by the program of the National Natural Science Foundation of China (grant Nos. 11573021, U1938104 and 12003020). We would like to thank the *TESS* science team for providing such excellent data.

Table 1. Basic Properties of GSC 4552-1498

Parameters	GSC 4552-1498	References
Brightness	12.655 mag	a
P	0.05581096 days	b
T_{eff}	7615 K	a
log g	4.34248 dex	a
B	13.047 mag	a
V	12.987 mag	a
J	12.395 mag	a
H	12.264 mag	a
K	12.228 mag	a
R	12.77 mag	a
Gaia	12.8319 mag	a
M_v	2.312 ± 0.263 mag	b
M_{bol}	2.344 ± 0.264 mag	b
L	$9.09 \pm 2.50\ L_{\odot}$	b
M	$1.68 \pm 0.10\ \mathrm{M}_{\odot}$	b

Note. — (a) These parameters are available in the TASOC; (b) Jafarzadeh & Poro (2017).

Table 2. Multi-frequency Solution of the Light Curves of GSC 4552-1498 (denoted by f_{Si}).

f_{Si}	Frequency (d^{-1})	Amplitude (mmag)	S/N	Identification
1	17.9176(7)	170.8	1042.4	F0
2	35.8352(2)	64.4	721.3	2F0
3	53.7529(1)	22.0	394.8	3F0
4	71.6705(2)	10.0	177.8	4F0
5	89.5882(1)	5.2	104.9	5F0
6	28.6803(5)	3.7	34.5	F2
7	46.5980(7)	1.8	25.1	F0+F2
8	22.6424(1)	0.9	10.9	F1
9	7.1546(1)	0.9	9.3	2F0-F2
10	64.5156(2)	0.8	14.1	2F0+F2
11	25.0722(2)	0.7	8.3	3F0-F2
12	10.7628(4)	0.7	10.2	F2-F0
13	82.4335(3)	0.5	9.2	3F0+F2

Note. — A total of 13 significant frequencies were detected, with S/N ratio larger than 4.0. Among these frequencies, there are 3 independent frequencies F0, F1 and F2, 4 harmonic frequencies and 6 combined frequencies.

Table 3. Candidate Models with $1/\chi^2 \geq 23$.

Mass ($M_\odot$)	Z (dex)	$\log T_{eff}$	$\log (L/L_\odot)$	$F0$ (c $days^{-1}$)	$F1$ (c $days^{-1}$)	$F2$ (c $days^{-1}$)	$(1/P)(dP/dt)$ (yr^{-1})	χ^2
1.13	0.006	3.8171	0.5614	17.6288	22.9287	28.6603	2.41×10^{-10}	0.0405
1.14	0.006	3.8195	0.5735	17.7673	22.9681	28.6803	2.46×10^{-10}	0.0390
1.15	0.006	3.8218	0.5870	17.9262	23.1307	28.6758	2.54×10^{-10}	0.0433
1.21	0.008	3.8168	0.5772	17.6455	22.9532	28.6697	3.09×10^{-10}	0.0419
1.22	0.008	3.8187	0.5909	17.7026	22.8119	28.5819	3.14×10^{-10}	0.0406
1.27	0.010	3.8187	0.6015	17.7375	22.8413	28.6874	2.74×10^{-10}	0.0412
1.28	0.010	3.8210	0.6142	17.7850	22.9575	28.6743	2.75×10^{-10}	0.0434
1.30	0.012	3.8189	0.6092	17.6775	22.8561	28.6280	2.65×10^{-10}	0.0422

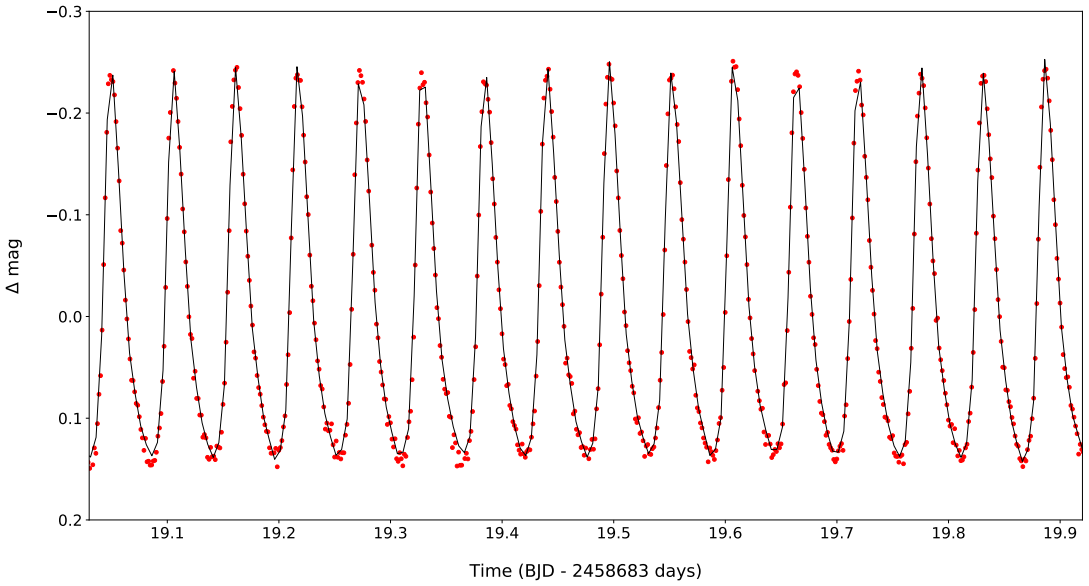

Fig. 1.— A 1-day section of the *TESS* light curve of GSC 4552-1498. The solid curves represent the fitting with the 13 frequency solutions listed in Table 2. BJD, barycentric Julian date.

Table 4. Physical Parameters of GSC 4552-1498 Derived from the Best-fitting Models.

Parameter	Values
$M(M_\odot)$	$1.14^{+0.16}_{-0.01}$
Z	$0.006^{+0.006}_{-0.000}$
T_{eff} (K)	6598^{+36}_{-40}
log $(L/L_\odot)$	$0.5735^{+0.0407}_{-0.0121}$

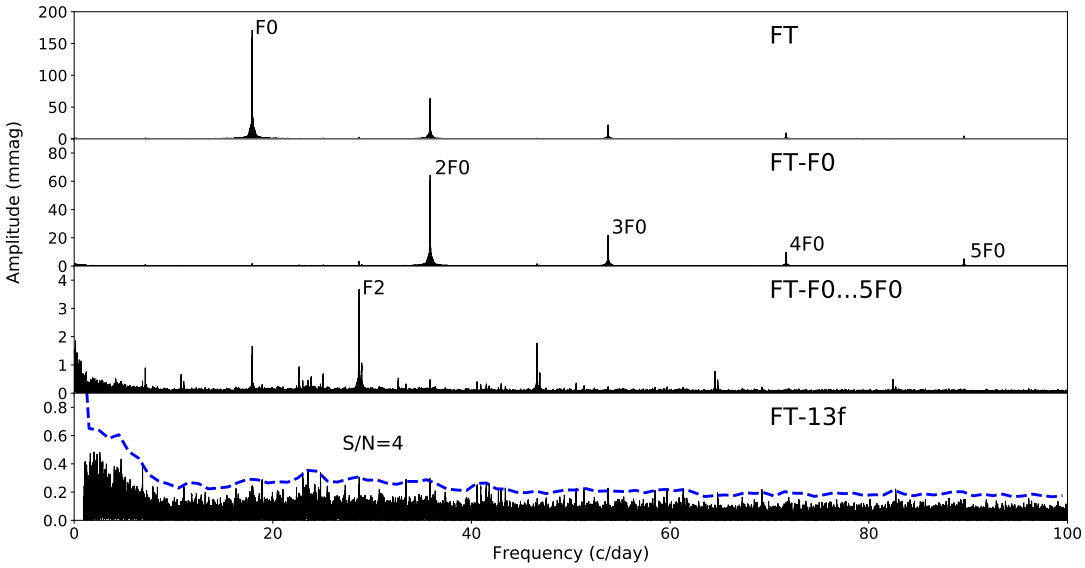

Fig. 2.— Fourier amplitude spectra of the frequency pre-whitening process for the light curves of GSC 4552-1498. Top panel, the initial Fourier amplitude spectra of the light curve, where the highest peak is F0=17.9176(7) d^{-1}. The second panel, amplitude spectra of the residuals after subtracting the F0, which shows 4 harmonic frequencies of F0. The third panel, amplitude spectra after subtracting the F0 and its harmonic frequencies, where the independent frequency F2 is marked. The bottom panel, it shows the residual after the fit shown in Table 2. Dotted curve refers to detection limit of S/N = 4.0.

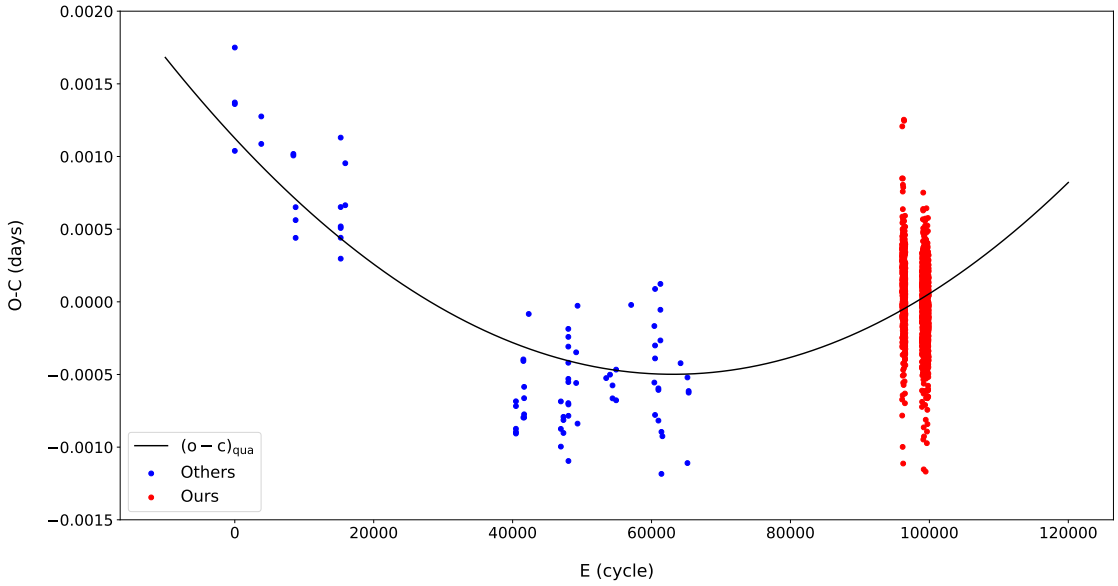

Fig. 3.— $O-C$ diagram of GSC 4552-1498, based on 1430 times of maximum light. The $O-C$ values are in days. Blue dots represent the previous 79 points and red dots are the 1351 new points. The black solid line shows the fit related to a continuously increasing period change.

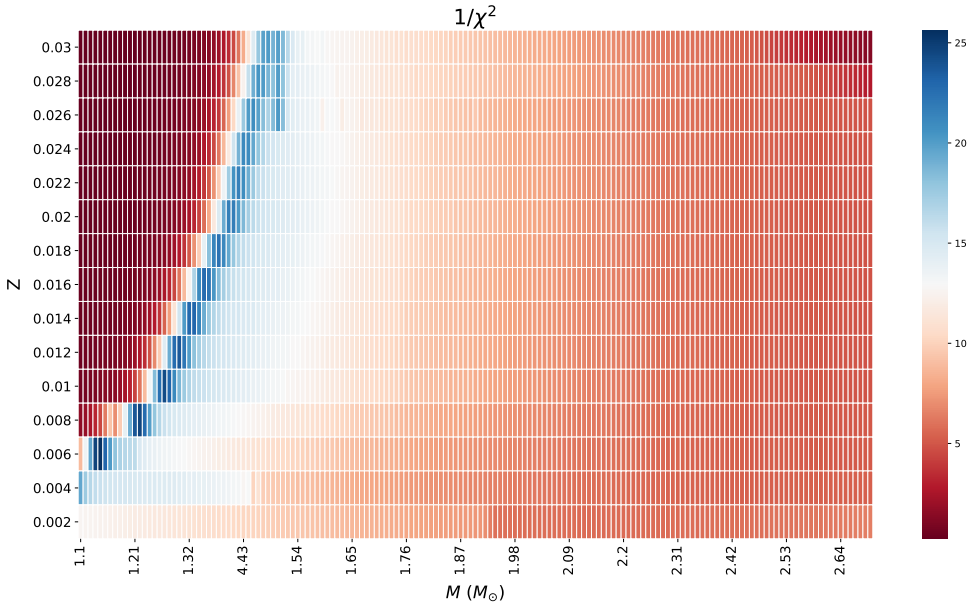

Fig. 4.— Probability distribution of $1/\chi^2$ values across the mass-metallicity plane. The bluer the color is, the smaller the value of χ^2 would be, which represents a higher probability to fit the observations. We note the mass-metallicity degeneracy is clear.

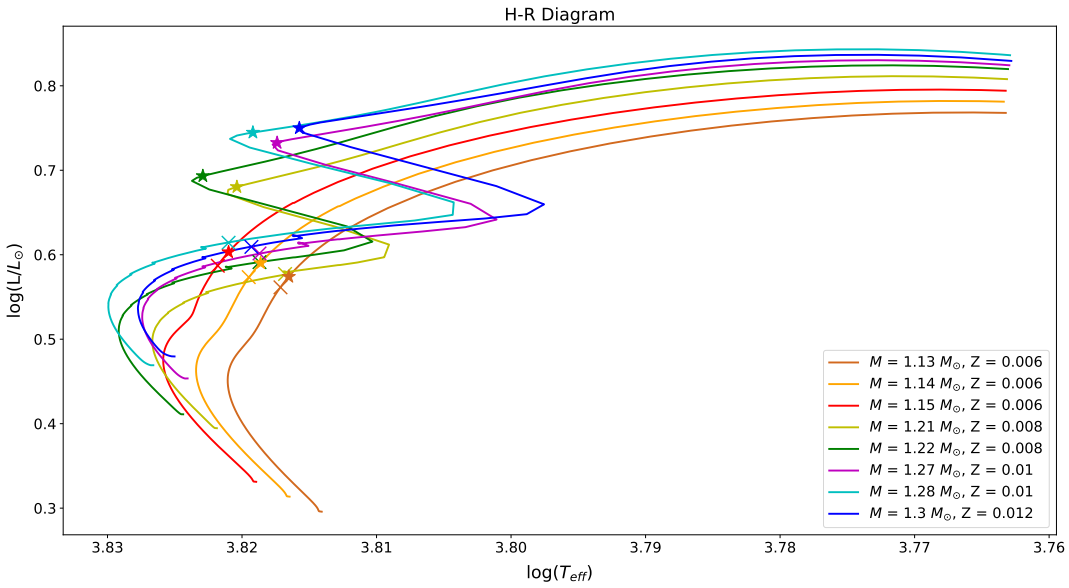

Fig. 5.— Evolutionary tracks from the zero-age MS to the post-MS across TAMS (star symbols) for the candidate models (color lines) in Table 3. The crosses mark the minimum χ^2 for each specific model by fitting the calculated $F0$, $F1$ and $F2$ with the observed values.

REFERENCES

Aerts, C., 2021, Rev.Mod.Phys., 93, 015001

Antoci, V., Cunha, M. S., Bowman, D. M., et al. 2019, MNRAS, 490, 4040

Balona, L. A. & Dziembowski, W. A. 2011, MNRAS, 417, 591

Balona, L. A., Lenz, P., Antoci, V., et al. 2012, MNRAS, 419, 3028

Balona, L. A. 2016, MNRAS, 459, 1097

Blake, R. M., Delaney, P., Khosravani, H., et al. 2003, PASP, 115, 212

Borucki, W. J., Koch, D., Basri, G., et al. 2010, Science, 327, 977

Bowman, D. M., Kurtz, D. W., Breger, M., et al. 2016, MNRAS, 460, 1970

Bowman, D. M. 2016, Ph.D. Thesis

Bowman, D. M., Hermans, J., Daszyńska-Daszkiewicz, J., et al. 2021, MNRAS, 504, 4039

Breger, M., Montgomery, M. H., 2014, ApJ, 783, 89

Breger, M., Stich, J., Garrido, R., et al. 1993, A&A, 271, 482

Breger, M. & Pamyatnykh, A. A. 1998, A&A, 332, 958

Breger, M. 2000, Delta Scuti and Related Stars, 210, 3

Chaplin, W. J., Appourchaux, T., Elsworth, Y., et al. 2010, ApJ, 713, L169

Chen, X., Li, Y., & Zhang, X. 2019, ApJ, 887, 253

Cox, J. P. & Giuli, R. T. 1968, PSS (New York: Gordon and Breach)

Fitch, W. S. & Szeidl, B. 1976, ApJ, 203, 616

Flower, P. J. 1996, ApJ, 469, 355

Fu, J. N., Khokhuntod, P., Rodríguez, E., et al. 2008, AJ, 135, 1958

Greiss, S., Steeghs, D., Gänsicke, B. T., et al. 2012, AJ, 144, 24

Handler, G., Pikall, H., & Diethelm, R. 1998, IBVS, 4549, 1

Henyey, L., Vardya, M. S., & Bodenheimer, P. 1965, ApJ, 142, 841

Hermans J., 2019, Master's thesis, Institute of Astronomy

Jafarzadeh, S. J. & Poro, A. 2017, New A, 54, 86

Jurcsik, J., Szeidl, B., Váradi, M., et al. 2006, A&A, 445, 617

Kjeldsen H., Christensen-Dalsgaard J., Handberg R., et al., 2010, AN, 331, 966

Koch, D. G., Borucki, W. J., Basri, G., et al. 2010, ApJ, 713, L79

Lee, Y.-H., Kim, S. S., Shin, J., et al. 2008, PASJ, 60, 551

Lenz P., Breger M. 2005, CoAst, 146, 53

Li, L.-J., Qian, S.-B., & Zhu, L.-Y. 2018, ApJ, 863, 151

McNamara, D. H. 2000, Delta Scuti and Related Stars, 210, 373

Montgomery, M. H. & Odonoghue, D. 1999, DSSN, 13, 28

Mow, B., Reinhart, E., Nhim, S., et al. 2016, AJ, 152, 17

Paxton, B., Bildsten, L., Dotter, A., et al. 2011, ApJS, 192, 3

Paxton, B., Cantiello, M., Arras, P., et al. 2013, ApJS, 208, 4

Paxton, B., Marchant, P., Schwab, J., et al. 2015, ApJS, 220, 15

Paxton, B., Schwab, J., Bauer, E. B., et al. 2018, ApJS, 234, 34

Paxton, B., Smolec, R., Schwab, J., et al. 2019, ApJS, 243, 10

Petersen, J. O. & Christensen-Dalsgaard, J. 1996, A&A, 312, 463

Poretti, E., Rainer, M., Weiss, W. W., et al. 2011, A&A, 528, A147

Qian, S.-B., Li, L.-J., He, J.-J., et al. 2018, MNRAS, 475, 478

Ricker, G. R., Winn, J. N., Vanderspek, R., et al. 2015, JATIS, 1, 014003

Rodríguez, E., and Breger, M., 2001, A&A, 366, 178

Rodríguez, E., López de Coca, P., Costa, V. and Martín, S., 1995, A&A, 299, 108

Stellingwerf, R. F. 1979, ApJ, 227, 935

Sterken, C., 2005, ASPC, 335, 3

Townsend, R. H. D. & Teitler, S. A. 2013, MNRAS, 435, 3406

Uytterhoeven, K., Moya, A., Grigahcène, A., et al. 2011, A&A, 534, A125

Watson, C., Henden, A. A., & Price, A. 2015, International Variable Star Index VSX, https://www.aavso.org/vsx

Wils, P., Rozakis, I., Kleidis, S., et al. 2008, A&A, 478, 865

Wils, P., Kleidis, S., Hambsch, F.-J., et al. 2009, IBVS, 5878, 1

Wils, P., Panagiotopoulos, K., van Wassenhove, J., et al. 2012, IBVS, 6015, 1

Wils, P., Ayiomamitis, A., Vanleenhove, M., et al. 2013, IBVS, 6049, 1

Wils, P., Ayiomamitis, A., Robertson, C. W., et al. 2014, IBVS, 6122, 1

Wils, P., Hambsch, F.-J., Vanleenhove, M., et al. 2015, IBVS, 6150, 1

Xue, H.-F., Fu, J.-N., Fox-Machado, L., et al. 2018, ApJ, 861, 96

Xue, H.-F. & Niu, J.-S. 2020, ApJ, 904, 5

Yang, X. H., Fu, J. N., & Zha, Q. 2012, AJ, 144, 92

Yang, T.-Z., Esamdin, A., Fu, J.-N., et al. 2018, RAA, 18, 002

Yang, T., Esamdin, A., Song, F., et al. 2018, ApJ, 863, 195

Yang, T.-Z. & Esamdin, A. 2019, ApJ, 879, 59

Yang, T.-Z., Sun, X.-Y., Zuo, Z.-Y., et al. 2021, AJ, 161, 27

Zhou, A.-Y. & Jiang, S.-Y. 2011, AJ, 142, 100

Ziaali, E., Bedding, T. R., Murphy, S. J., Van Reeth, T., Hey, D. R., 2019, MNRAS, 486, 4348

Appendix

This preprint was prepared with the AAS LaTeX macros v5.2.

Table A1. 1351 New Times of Maximum Light and $O-C$ Values of GSC 4552-1498.

BJD (2450000+)	*E*	$O-C$ (day)	*BJD* (2450000+)	*E*	$O-C$ (day)	*BJD* (2450000+)	*E*	$O-C$ (day)
8683.4103	96072	0.000393	8709.6410	96542	–0.000080	8868.8146	99394	0.000524
8683.4657	96073	–0.000018	8709.6968	96543	–0.000091	8870.9350	99432	0.000106
8683.5219	96074	0.000371	8709.7527	96544	–0.000002	8870.9907	99433	–0.000005
8683.5777	96075	0.000360	8709.8085	96545	–0.000013	8871.0467	99434	0.000184
8683.6340	96076	0.000849	8709.8640	96546	–0.000324	8871.1029	99435	0.000573
8683.6892	96077	0.000238	8709.9204	96547	0.000265	8871.1584	99436	0.000262
8683.7441	96078	–0.000673	8709.9757	96548	–0.000247	8871.2135	99437	–0.000449
8683.8009	96079	0.000316	8710.0316	96549	–0.000158	8871.2695	99438	–0.000260
8683.8563	96080	–0.000095	8710.0878	96550	0.000231	8871.3257	99439	0.000129
8683.9124	96081	0.000194	8710.1431	96551	–0.000280	8871.3813	99440	–0.000082
8683.9683	96082	0.000283	8842.5273	98923	0.000209	8871.4369	99441	–0.000293
8684.0239	96083	0.000072	8842.5828	98924	–0.000102	8871.4931	99442	0.000096
8684.0800	96084	0.000361	8842.6383	98925	–0.000413	8871.5484	99443	–0.000415
8684.1356	96085	0.000150	8842.6947	98926	0.000176	8871.6045	99444	–0.000126
8684.1916	96086	0.000339	8842.8057	98928	–0.000446	8871.6606	99445	0.000163
8684.2472	96087	0.000128	8842.8615	98929	–0.000457	8871.7159	99446	–0.000348
8684.3021	96088	–0.000783	8842.9175	98930	–0.000268	8871.7720	99447	–0.000059
8684.3590	96089	0.000306	8842.9733	98931	–0.000279	8871.8275	99448	–0.000370
8684.4144	96090	–0.000105	8843.0295	98932	0.000110	8871.8836	99449	–0.000081
8684.4706	96091	0.000284	8843.0849	98933	–0.000301	8871.9398	99450	0.000308
8684.5264	96092	0.000273	8843.1410	98934	–0.000012	8871.9948	99451	–0.000503
8684.5819	96093	–0.000038	8843.1961	98935	–0.000723	8872.0511	99452	–0.000014
8684.6382	96094	0.000451	8843.2525	98936	–0.000134	8872.1067	99453	–0.000225
8684.6935	96095	–0.000060	8843.3083	98937	–0.000145	8872.1624	99454	–0.000336
8684.7497	96096	0.000329	8843.3639	98938	–0.000356	8872.2186	99455	0.000053
8684.8055	96097	0.000318	8843.4200	98939	–0.000067	8872.2739	99456	–0.000458
8684.8622	96098	0.001207	8843.4756	98940	–0.000278	8872.3306	99457	0.000431
8684.9171	96099	0.000296	8843.5318	98941	0.000111	8872.3860	99458	0.000020
8684.9725	96100	–0.000115	8843.5876	98942	0.000100	8872.4417	99459	–0.000091
8685.0285	96101	0.000074	8843.6427	98943	–0.000611	8872.4977	99460	0.000098
8685.0843	96102	0.000063	8843.6991	98944	–0.000022	8872.5533	99461	–0.000113

Table A1—Continued

BJD (2450000+)	*E*	*O*−*C* (day)	*BJD* (2450000+)	*E*	*O*−*C* (day)	*BJD* (2450000+)	*E*	*O*−*C* (day)
8685.1398	96103	–0.000248	8843.7546	98945	–0.000333	8872.6095	99462	0.000276
8685.1961	96104	0.000241	8843.8105	98946	–0.000244	8872.6650	99463	–0.000035
8685.2515	96105	–0.000170	8843.8663	98947	–0.000255	8872.7208	99464	–0.000046
8685.3076	96106	0.000119	8843.9220	98948	–0.000366	8872.7770	99465	0.000343
8685.3634	96107	0.000108	8843.9783	98949	0.000123	8872.8313	99466	–0.001168
8685.4188	96108	–0.000303	8844.0333	98950	–0.000688	8872.8885	99467	0.000221
8685.4755	96109	0.000586	8844.0898	98951	0.000001	8872.9439	99468	–0.000190
8685.5307	96110	–0.000025	8844.1453	98952	–0.000310	8873.0000	99469	0.000099
8685.5866	96111	0.000064	8844.2012	98953	–0.000221	8873.0558	99470	0.000088
8685.6426	96112	0.000253	8844.2572	98954	–0.000032	8873.1111	99471	–0.000423
8685.6982	96113	0.000042	8844.3129	98955	–0.000143	8873.1674	99472	0.000066
8685.7542	96114	0.000231	8844.3686	98956	–0.000254	8873.2229	99473	–0.000245
8685.8095	96115	–0.000280	8844.4250	98957	0.000335	8873.2786	99474	–0.000356
8685.8658	96116	0.000209	8844.4806	98958	0.000124	8873.3348	99475	0.000033
8685.9218	96117	0.000398	8844.5365	98959	0.000213	8873.3902	99476	–0.000378
8685.9769	96118	–0.000313	8844.5921	98960	0.000002	8873.4464	99477	0.000011
8686.0334	96119	0.000376	8844.6478	98961	–0.000109	8873.5018	99478	–0.000400
8686.0888	96120	–0.000035	8844.7039	98962	0.000180	8873.5572	99479	–0.000811
8686.1444	96121	–0.000246	8844.7595	98963	–0.000031	8873.6138	99480	–0.000023
8686.2010	96122	0.000543	8844.8155	98964	0.000158	8873.6693	99481	–0.000334
8686.2565	96123	0.000232	8844.8712	98965	0.000047	8873.7252	99482	–0.000245
8686.3123	96124	0.000221	8844.9271	98966	0.000136	8873.7808	99483	–0.000456
8686.3681	96125	0.000210	8844.9829	98967	0.000125	8873.8366	99484	–0.000467
8686.4237	96126	–0.000001	8845.0387	98968	0.000114	8873.8931	99485	0.000222
8686.4798	96127	0.000288	8845.0947	98969	0.000303	8873.9486	99486	–0.000089
8686.5354	96128	0.000077	8845.1501	98970	–0.000108	8874.0048	99487	0.000300
8686.5913	96129	0.000166	8845.2061	98971	0.000081	8874.0603	99488	–0.000011
8686.6471	96130	0.000155	8845.2621	98972	0.000270	8874.1160	99489	–0.000122
8686.7029	96131	0.000144	8845.3176	98973	–0.000041	8874.1721	99490	0.000167
8686.7590	96132	0.000433	8845.3737	98974	0.000248	8874.2278	99491	0.000056
8686.8141	96133	–0.000278	8845.4296	98975	0.000337	8874.2837	99492	0.000145
8686.8705	96134	0.000311	8845.4851	98976	0.000026	8874.3393	99493	–0.000066

Table A1—Continued

BJD (2450000+)	*E*	*O*−*C* (day)	*BJD* (2450000+)	*E*	*O*−*C* (day)	*BJD* (2450000+)	*E*	*O*−*C* (day)
8686.9261	96135	0.000100	8845.5411	98977	0.000215	8874.3953	99494	0.000123
8686.9819	96136	0.000089	8845.5966	98978	–0.000096	8874.4511	99495	0.000112
8687.0379	96137	0.000278	8845.6528	98979	0.000293	8874.5067	99496	–0.000099
8687.0935	96138	0.000067	8845.7083	98980	–0.000018	8874.5628	99497	0.000190
8687.1496	96139	0.000356	8845.7642	98981	0.000071	8874.6185	99498	0.000079
8687.2049	96140	–0.000155	8845.8199	98982	–0.000040	8874.6743	99499	0.000068
8687.2611	96141	0.000234	8845.8759	98983	0.000149	8874.7301	99500	0.000057
8687.3171	96142	0.000423	8845.9318	98984	0.000238	8874.7856	99501	–0.000254
8687.3726	96143	0.000112	8845.9872	98985	–0.000173	8874.8418	99502	0.000135
8687.4288	96144	0.000501	8846.0433	98986	0.000116	8874.8975	99503	0.000024
8687.4838	96145	–0.000310	8846.0992	98987	0.000205	8874.9529	99504	–0.000387
8687.5959	96147	0.000168	8846.1543	98988	–0.000506	8875.0090	99505	–0.000098
8687.6509	96148	–0.000643	8846.2105	98989	–0.000117	8875.0645	99506	–0.000409
8687.7076	96149	0.000246	8846.2663	98990	–0.000128	8875.1206	99507	–0.000120
8687.7628	96150	–0.000365	8846.3221	98991	–0.000140	8875.1764	99508	–0.000131
8687.8191	96151	0.000124	8846.3781	98992	0.000049	8875.2321	99509	–0.000242
8687.8750	96152	0.000213	8846.4339	98993	0.000038	8875.2881	99510	–0.000053
8687.9296	96153	–0.000998	8846.4900	98994	0.000327	8875.3437	99511	–0.000264
8687.9868	96154	0.000391	8846.5454	98995	–0.000084	8875.3996	99512	–0.000175
8688.0425	96155	0.000280	8846.6014	98996	0.000105	8875.4552	99513	–0.000386
8688.0981	96156	0.000069	8846.6573	98997	0.000194	8875.5112	99514	–0.000197
8688.1541	96157	0.000258	8846.7129	98998	–0.000017	8875.5670	99515	–0.000208
8688.2097	96158	0.000047	8846.7690	98999	0.000272	8875.6226	99516	–0.000419
8688.2658	96159	0.000336	8846.8243	99000	–0.000239	8875.6789	99517	0.000070
8688.3213	96160	0.000025	8846.8804	99001	0.000050	8875.7344	99518	–0.000241
8688.3772	96161	0.000114	8846.9362	99002	0.000039	8875.7902	99519	–0.000252
8688.4327	96162	–0.000197	8846.9919	99003	–0.000072	8875.8464	99520	0.000137
8688.4882	96163	–0.000508	8847.0481	99004	0.000317	8875.9018	99521	–0.000274
8688.5449	96164	0.000381	8847.1034	99005	–0.000194	8875.9579	99522	0.000015
8688.6004	96165	0.000070	8847.1595	99006	0.000095	8876.0132	99523	–0.000496
8688.6569	96166	0.000759	8847.2154	99007	0.000184	8876.0693	99524	–0.000207
8688.7125	96167	0.000548	8847.2708	99008	–0.000227	8876.1255	99525	0.000182

Table A1—Continued

BJD (2450000+)	*E*	*O*−*C* (day)	*BJD* (2450000+)	*E*	*O*−*C* (day)	*BJD* (2450000+)	*E*	*O*−*C* (day)
8688.7675	96168	–0.000263	8847.3271	99009	0.000262	8876.1806	99526	–0.000529
8688.8240	96169	0.000426	8847.3826	99010	–0.000049	8876.2369	99527	–0.000040
8688.8794	96170	0.000015	8847.4386	99011	0.000140	8876.2928	99528	0.000049
8688.9354	96171	0.000204	8847.4945	99012	0.000229	8876.3479	99529	–0.000662
8688.9915	96172	0.000493	8847.5499	99013	–0.000182	8876.4048	99530	0.000427
8689.0469	96173	0.000082	8847.6061	99014	0.000207	8876.4599	99531	–0.000284
8689.1031	96174	0.000471	8847.6617	99015	–0.000004	8876.5158	99532	–0.000195
8689.1584	96175	–0.000040	8847.7175	99016	–0.000015	8876.5717	99533	–0.000106
8689.2151	96176	0.000849	8847.7736	99017	0.000274	8876.6272	99534	–0.000417
8689.2707	96177	0.000638	8847.8291	99018	–0.000037	8876.6837	99535	0.000272
8689.3257	96178	–0.000173	8847.8850	99019	0.000052	8876.7388	99536	–0.000439
8689.3820	96179	0.000316	8847.9407	99020	–0.000059	8876.7950	99537	–0.000050
8689.4375	96180	0.000005	8847.9967	99021	0.000130	8876.8510	99538	0.000139
8689.4933	96181	–0.000006	8848.0526	99022	0.000219	8876.9065	99539	–0.000172
8689.5495	96182	0.000382	8848.1081	99023	–0.000092	8876.9629	99540	0.000417
8689.6048	96183	–0.000129	8848.1642	99024	0.000197	8877.0181	99541	–0.000194
8689.6611	96184	0.000360	8848.2199	99025	0.000086	8877.0744	99542	0.000295
8689.7166	96185	0.000049	8848.2755	99026	–0.000125	8877.1301	99543	0.000184
8689.7725	96186	0.000138	8848.3316	99027	0.000164	8877.1857	99544	–0.000027
8689.8282	96187	0.000027	8848.3873	99028	0.000053	8877.2419	99545	0.000362
8689.8840	96188	0.000016	8848.4434	99029	0.000342	8877.2977	99546	0.000351
8689.9406	96189	0.000805	8848.4989	99030	0.000031	8877.3532	99547	0.000040
8689.9955	96190	–0.000106	8848.5547	99031	0.000020	8877.4090	99548	0.000029
8690.0514	96191	–0.000017	8848.6108	99032	0.000309	8877.4645	99549	–0.000282
8690.1078	96192	0.000572	8848.6664	99033	0.000098	8877.5208	99550	0.000207
8690.1628	96193	–0.000239	8848.7222	99034	0.000087	8877.5763	99551	–0.000104
8690.2189	96194	0.000050	8848.7780	99035	0.000076	8877.6324	99552	0.000185
8690.2749	96195	0.000239	8848.8339	99036	0.000165	8877.6882	99553	0.000174
8690.3306	96196	0.000128	8848.8895	99037	–0.000046	8877.7441	99554	0.000263
8690.3862	96197	–0.000083	8848.9454	99038	0.000043	8877.7999	99555	0.000252
8690.4418	96198	–0.000294	8849.0014	99039	0.000232	8877.8554	99556	–0.000059
8690.4979	96199	–0.000005	8849.0569	99040	–0.000079	8877.9112	99557	–0.000070

Table A1—Continued

BJD (2450000+)	*E*	*O*−*C* (day)	*BJD* (2450000+)	*E*	*O*−*C* (day)	*BJD* (2450000+)	*E*	*O*−*C* (day)
8690.5535	96200	–0.000216	8849.1129	99041	0.000110	8877.9670	99558	–0.000081
8690.6093	96201	–0.000227	8849.1686	99042	–0.000001	8878.0225	99559	–0.000392
8690.6653	96202	–0.000038	8849.2243	99043	–0.000112	8878.0787	99560	–0.000003
8690.7209	96203	–0.000249	8849.2805	99044	0.000277	8878.1342	99561	–0.000314
8690.7769	96204	–0.000060	8849.3360	99045	–0.000034	8878.1903	99562	–0.000025
8690.8326	96205	–0.000171	8849.3920	99046	0.000155	8878.2461	99563	–0.000036
8690.8887	96206	0.000118	8849.4478	99047	0.000144	8878.3018	99564	–0.000147
8690.9447	96207	0.000307	8849.5036	99048	0.000133	8878.3577	99565	–0.000058
8691.0002	96208	–0.000004	8849.5595	99049	0.000222	8878.4131	99566	–0.000469
8691.0564	96209	0.000385	8849.6150	99050	–0.000089	8878.4694	99567	0.000020
8691.1120	96210	0.000174	8849.6711	99051	0.000200	8878.5250	99568	–0.000191
8691.1679	96211	0.000263	8849.7265	99052	–0.000211	8878.5806	99569	–0.000402
8691.2236	96212	0.000152	8849.7823	99053	–0.000222	8878.6368	99570	–0.000013
8691.2793	96213	0.000041	8849.8384	99054	0.000067	8878.6923	99571	–0.000324
8691.3353	96214	0.000230	8849.8940	99055	–0.000144	8878.7484	99572	–0.000035
8691.3907	96215	–0.000181	8849.9501	99056	0.000145	8878.8040	99573	–0.000246
8691.4464	96216	–0.000292	8850.0059	99057	0.000134	8878.8599	99574	–0.000157
8691.5025	96217	–0.000003	8850.0613	99058	–0.000277	8878.9161	99575	0.000232
8691.5582	96218	–0.000114	8850.1177	99059	0.000312	8878.9713	99576	–0.000379
8691.6144	96219	0.000275	8850.1732	99060	0.000001	8879.0276	99577	0.000110
8691.6699	96220	–0.000036	8850.2290	99061	–0.000010	8879.0834	99578	0.000099
8691.7259	96221	0.000153	8850.2846	99062	–0.000221	8879.1388	99579	–0.000312
8691.7820	96222	0.000442	8850.3412	99063	0.000568	8879.1954	99580	0.000477
8691.8369	96223	–0.000469	8850.3963	99064	–0.000143	8879.2504	99581	–0.000334
8691.8934	96224	0.000220	8850.4519	99065	–0.000354	8879.3067	99582	0.000155
8691.9491	96225	0.000109	8850.5079	99066	–0.000165	8879.3630	99583	0.000644
8692.0048	96226	–0.000002	8850.5639	99067	0.000024	8879.4180	99584	–0.000167
8692.0595	96227	–0.001113	8850.6192	99068	–0.000487	8879.4743	99585	0.000322
8692.1160	96228	–0.000424	8850.6755	99069	0.000002	8879.5296	99586	–0.000189
8692.1725	96229	0.000265	8850.7309	99070	–0.000409	8879.5858	99587	0.000200
8692.2278	96230	–0.000246	8850.7872	99071	0.000080	8879.6415	99588	0.000089
8692.2833	96231	–0.000557	8850.8429	99072	–0.000031	8879.6971	99589	–0.000122

Table A1—Continued

BJD (2450000+)	*E*	*O*−*C* (day)	*BJD* (2450000+)	*E*	*O*−*C* (day)	*BJD* (2450000+)	*E*	*O*−*C* (day)
8692.3396	96232	–0.000068	8850.8991	99073	0.000358	8879.7534	99590	0.000367
8692.4513	96234	0.000010	8850.9547	99074	0.000147	8879.8085	99591	–0.000344
8692.5070	96235	–0.000101	8851.0099	99075	–0.000464	8879.8648	99592	0.000145
8692.5637	96236	0.000788	8851.0659	99076	–0.000275	8879.9207	99593	0.000234
8692.6189	96237	0.000177	8851.1220	99077	0.000014	8879.9759	99594	–0.000377
8692.6745	96238	–0.000034	8851.1773	99078	–0.000497	8880.0325	99595	0.000412
8692.7306	96239	0.000255	8851.2337	99079	0.000092	8880.0877	99596	–0.000199
8692.7863	96240	0.000144	8851.2892	99080	–0.000219	8880.1442	99597	0.000490
8692.8419	96241	–0.000067	8851.3451	99081	–0.000130	8880.1997	99598	0.000179
8692.8980	96242	0.000222	8851.4010	99082	–0.000041	8880.2552	99599	–0.000132
8692.9537	96243	0.000111	8851.4567	99083	–0.000152	8880.3114	99600	0.000257
8693.0098	96244	0.000400	8851.5130	99084	0.000337	8880.3669	99601	–0.000054
8693.0655	96245	0.000289	8851.5684	99085	–0.000074	8880.4230	99602	0.000234
8693.1210	96246	–0.000022	8851.6242	99086	–0.000085	8880.4787	99603	0.000123
8693.1771	96247	0.000267	8851.6804	99087	0.000304	8880.5340	99604	–0.000388
8693.2325	96248	–0.000144	8851.7359	99088	–0.000007	8880.5906	99605	0.000401
8693.2887	96249	0.000245	8851.7919	99089	0.000182	8880.6459	99606	–0.000110
8693.3442	96250	–0.000066	8851.8472	99090	–0.000329	8880.7016	99607	–0.000221
8693.4004	96251	0.000323	8851.9033	99091	–0.000040	8880.7580	99608	0.000368
8693.4562	96252	0.000312	8851.9595	99092	0.000349	8880.8133	99609	–0.000143
8693.5118	96253	0.000101	8852.0148	99093	–0.000162	8880.8693	99610	0.000046
8693.5676	96254	0.000090	8852.0708	99094	0.000027	8880.9248	99611	–0.000265
8693.6237	96255	0.000379	8852.1267	99095	0.000116	8880.9808	99612	–0.000076
8693.6793	96256	0.000168	8852.1826	99096	0.000205	8881.0367	99613	0.000013
8693.7355	96257	0.000557	8852.2382	99097	–0.000006	8881.0921	99614	–0.000398
8693.7907	96258	–0.000054	8852.2938	99098	–0.000217	8881.1484	99615	0.000091
8693.8469	96259	0.000335	8852.3498	99099	–0.000028	8881.2040	99616	–0.000120
8693.9024	96260	0.000024	8852.4055	99100	–0.000139	8881.2598	99617	–0.000131
8693.9583	96261	0.000113	8852.4614	99101	–0.000050	8881.3157	99618	–0.000042
8694.0143	96262	0.000302	8852.5179	99102	0.000639	8881.3714	99619	–0.000153
8694.0698	96263	–0.000009	8852.5730	99103	–0.000072	8881.4274	99620	0.000036
8694.1259	96264	0.000280	8852.6293	99104	0.000417	8881.4832	99621	0.000025

Table A1—Continued

BJD (2450000+)	*E*	*O*−*C* (day)	*BJD* (2450000+)	*E*	*O*−*C* (day)	*BJD* (2450000+)	*E*	*O*−*C* (day)
8694.1815	96265	0.000069	8852.6850	99105	0.000306	8881.5387	99622	–0.000286
8694.2372	96266	–0.000042	8852.7407	99106	0.000195	8881.5948	99623	0.000003
8694.2934	96267	0.000347	8852.7968	99107	0.000484	8881.6503	99624	–0.000308
8694.3489	96268	0.000036	8852.8526	99108	0.000473	8881.7064	99625	–0.000019
8694.4047	96269	0.000025	8852.9083	99109	0.000362	8881.7620	99626	–0.000230
8694.4608	96270	0.000314	8852.9633	99110	–0.000449	8881.8178	99627	–0.000241
8694.5165	96271	0.000203	8853.0198	99111	0.000240	8881.8736	99628	–0.000252
8694.5725	96272	0.000392	8853.0760	99112	0.000629	8881.9293	99629	–0.000363
8694.6279	96273	–0.000019	8853.1314	99113	0.000218	8881.9851	99630	–0.000374
8694.6839	96274	0.000170	8853.1875	99114	0.000506	8882.0411	99631	–0.000185
8694.7398	96275	0.000259	8853.2431	99115	0.000295	8882.0970	99632	–0.000096
8694.7955	96276	0.000148	8853.3548	99117	0.000373	8882.1529	99633	–0.000007
8694.8516	96277	0.000437	8853.4102	99118	–0.000038	8882.2085	99634	–0.000218
8694.9071	96278	0.000126	8853.4668	99119	0.000751	8882.2646	99635	0.000071
8694.9631	96279	0.000315	8853.5218	99120	–0.000060	8882.3199	99636	–0.000440
8695.0186	96280	0.000004	8853.5777	99121	0.000029	8882.3763	99637	0.000149
8695.0745	96281	0.000093	8853.6339	99122	0.000418	8882.4320	99638	0.000038
8695.1305	96282	0.000282	8853.6893	99123	0.000007	8882.4868	99639	–0.000973
8695.1862	96283	0.000171	8853.7453	99124	0.000196	8882.5438	99640	0.000216
8695.2420	96284	0.000160	8853.8006	99125	–0.000315	8882.5992	99641	–0.000195
8695.2978	96285	0.000149	8853.8568	99126	0.000074	8882.6554	99642	0.000194
8695.3537	96286	0.000238	8853.9127	99127	0.000163	8882.7112	99643	0.000183
8695.4094	96287	0.000127	8853.9674	99128	–0.000948	8882.7667	99644	–0.000128
8695.4649	96288	–0.000184	8854.0243	99129	0.000141	8882.8224	99645	–0.000239
8695.5212	96289	0.000305	8854.0797	99130	–0.000270	8882.8781	99646	–0.000350
8695.5770	96290	0.000294	8854.1357	99131	–0.000081	8882.9345	99647	0.000239
8695.6329	96291	0.000383	8854.1918	99132	0.000208	8882.9902	99648	0.000128
8695.6885	96292	0.000172	8854.2471	99133	–0.000303	8883.0457	99649	–0.000183
8695.7439	96293	–0.000239	8854.3034	99134	0.000186	8883.1020	99650	0.000306
8695.8003	96294	0.000350	8854.3589	99135	–0.000125	8883.1573	99651	–0.000205
8695.8559	96295	0.000139	8854.4143	99136	–0.000536	8883.2134	99652	0.000084
8695.9110	96296	–0.000572	8854.4709	99137	0.000253	8883.2693	99653	0.000173

Table A1—Continued

BJD (2450000+)	*E*	*O*−*C* (day)	*BJD* (2450000+)	*E*	*O*−*C* (day)	*BJD* (2450000+)	*E*	*O*−*C* (day)
8695.9678	96297	0.000417	8854.5264	99138	–0.000058	8883.3249	99654	–0.000038
8696.0231	96298	–0.000094	8854.5823	99139	0.000031	8883.3811	99655	0.000351
8696.0793	96299	0.000295	8854.6382	99140	0.000120	8883.4365	99656	–0.000060
8696.1348	96300	–0.000016	8854.6940	99141	0.000109	8883.4925	99657	0.000129
8696.1904	96301	–0.000227	8854.7499	99142	0.000198	8883.5481	99658	–0.000082
8696.2467	96302	0.000262	8854.8053	99143	–0.000213	8883.6031	99659	–0.000893
8696.3022	96303	–0.000049	8856.4234	99172	–0.000632	8883.6601	99660	0.000296
8696.3585	96304	0.000439	8856.5358	99174	0.000146	8883.7155	99661	–0.000115
8697.3631	96322	0.000441	8856.5915	99175	0.000035	8883.7715	99662	0.000074
8697.4182	96323	–0.000270	8856.6469	99176	–0.000376	8883.8274	99663	0.000163
8697.4744	96324	0.000119	8856.7027	99177	–0.000387	8883.8824	99664	–0.000648
8697.5301	96325	0.000008	8856.7589	99178	0.000002	8883.9388	99665	–0.000059
8697.5854	96326	–0.000503	8856.8145	99179	–0.000209	8885.7807	99698	0.000078
8697.6420	96327	0.000286	8856.8705	99180	–0.000020	8885.8365	99699	0.000067
8697.6976	96328	0.000075	8856.9263	99181	–0.000031	8885.8925	99700	0.000256
8697.7533	96329	–0.000036	8856.9821	99182	–0.000042	8885.9477	99701	–0.000355
8697.8104	96330	0.001253	8857.0368	99183	–0.001153	8886.0039	99702	0.000034
8697.8645	96331	–0.000458	8857.0929	99184	–0.000864	8886.0598	99703	0.000123
8697.9210	96332	0.000231	8857.1492	99185	–0.000375	8886.1154	99704	–0.000088
8697.9765	96333	–0.000080	8857.2055	99186	0.000114	8886.1715	99705	0.000201
8698.0325	96334	0.000109	8857.2610	99187	–0.000197	8886.2268	99706	–0.000310
8698.0883	96335	0.000098	8857.3170	99188	–0.000008	8886.2831	99707	0.000179
8698.1439	96336	–0.000113	8857.3731	99189	0.000281	8886.3389	99708	0.000168
8698.1999	96337	0.000076	8857.4288	99190	0.000170	8886.3938	99709	–0.000743
8698.2557	96338	0.000065	8857.4845	99191	0.000059	8886.4507	99710	0.000346
8698.3113	96339	–0.000146	8857.5405	99192	0.000248	8886.5057	99711	–0.000465
8698.3674	96340	0.000143	8857.5955	99193	–0.000563	8886.5618	99712	–0.000176
8698.4229	96341	–0.000168	8857.6517	99194	–0.000174	8886.6180	99713	0.000213
8698.4790	96342	0.000121	8857.7074	99195	–0.000285	8886.6735	99714	–0.000098
8698.5348	96343	0.000110	8857.7632	99196	–0.000296	8886.7288	99715	–0.000609
8698.5907	96344	0.000199	8857.8194	99197	0.000093	8886.7852	99716	–0.000020
8698.6466	96345	0.000288	8857.8749	99198	–0.000218	8886.8407	99717	–0.000331

Table A1—Continued

BJD (2450000+)	*E*	*O*−*C* (day)	*BJD* (2450000+)	*E*	*O*−*C* (day)	*BJD* (2450000+)	*E*	*O*−*C* (day)
8698.7021	96346	–0.000023	8857.9310	99199	0.000071	8886.8970	99718	0.000158
8698.7584	96347	0.000466	8857.9866	99200	–0.000140	8886.9525	99719	–0.000153
8698.8136	96348	–0.000145	8858.0424	99201	–0.000151	8887.0086	99720	0.000136
8698.8698	96349	0.000244	8858.0984	99202	0.000038	8887.0648	99721	0.000525
8698.9255	96350	0.000133	8858.1539	99203	–0.000273	8887.1201	99722	0.000014
8698.9813	96351	0.000122	8858.2100	99204	0.000016	8887.1762	99723	0.000303
8699.0374	96352	0.000411	8858.2655	99205	–0.000295	8887.2314	99724	–0.000309
8699.0928	96353	0.000000	8858.3213	99206	–0.000306	8887.2878	99725	0.000280
8699.1490	96354	0.000389	8858.3778	99207	0.000383	8887.3429	99726	–0.000431
8699.2046	96355	0.000178	8858.4329	99208	–0.000328	8887.3983	99727	–0.000842
8699.2603	96356	0.000067	8858.4888	99209	–0.000239	8887.4549	99728	–0.000053
8699.3166	96357	0.000556	8858.5452	99210	0.000350	8887.5101	99729	–0.000664
8699.3719	96358	0.000045	8858.6008	99211	0.000139	8887.5667	99730	0.000125
8699.4279	96359	0.000234	8858.6564	99212	–0.000072	8887.6223	99731	–0.000086
8699.4836	96360	0.000123	8858.7120	99213	–0.000283	8887.6783	99732	0.000103
8699.5391	96361	–0.000188	8858.7681	99214	0.000006	8887.7339	99733	–0.000108
8699.5953	96362	0.000201	8858.8237	99215	–0.000205	8887.7894	99734	–0.000419
8699.6509	96363	–0.000010	8858.8796	99216	–0.000116	8887.8456	99735	–0.000030
8699.7072	96364	0.000479	8858.9358	99217	0.000273	8887.9014	99736	–0.000041
8699.7628	96365	0.000268	8858.9912	99218	–0.000138	8887.9571	99737	–0.000152
8699.8185	96366	0.000157	8859.0468	99219	–0.000349	8888.0134	99738	0.000337
8699.8754	96367	0.001246	8859.1029	99220	–0.000060	8888.0688	99739	–0.000074
8699.9299	96368	–0.000065	8859.1587	99221	–0.000071	8888.1248	99740	0.000115
8699.9860	96369	0.000224	8859.2147	99222	0.000118	8888.1809	99741	0.000404
8700.0418	96370	0.000213	8859.2703	99223	–0.000093	8888.2364	99742	0.000093
8700.0974	96371	0.000002	8859.3259	99224	–0.000304	8888.2925	99743	0.000382
8700.1535	96372	0.000291	8859.3820	99225	–0.000015	8888.3478	99744	–0.000129
8700.2092	96373	0.000180	8859.4369	99226	–0.000926	8888.4039	99745	0.000160
8700.2650	96374	0.000169	8859.4936	99227	–0.000037	8888.4597	99746	0.000149
8700.3210	96375	0.000358	8859.5494	99228	–0.000048	8888.5149	99747	–0.000462
8700.3761	96376	–0.000353	8859.6053	99229	0.000041	8888.5712	99748	0.000027
8700.4327	96377	0.000436	8859.6609	99230	–0.000170	8888.6265	99749	–0.000484

Table A1—Continued

BJD (2450000+)	*E*	*O*−*C* (day)	*BJD* (2450000+)	*E*	*O*−*C* (day)	*BJD* (2450000+)	*E*	*O*−*C* (day)
8700.4882	96378	0.000125	8859.7167	99231	–0.000181	8888.6829	99750	0.000105
8700.5439	96379	0.000014	8859.7727	99232	0.000008	8888.7386	99751	–0.000006
8700.6000	96380	0.000303	8859.8283	99233	–0.000203	8888.7943	99752	–0.000117
8700.6557	96381	0.000192	8859.8845	99234	0.000186	8888.8506	99753	0.000372
8700.7117	96382	0.000381	8859.9402	99235	0.000075	8888.9061	99754	0.000061
8700.7671	96383	–0.000030	8859.9956	99236	–0.000337	8888.9619	99755	0.000050
8700.8229	96384	–0.000041	8860.0520	99237	0.000252	8889.0178	99756	0.000139
8700.8790	96385	0.000248	8860.1071	99238	–0.000459	8889.0734	99757	–0.000072
8700.9342	96386	–0.000363	8860.1635	99239	0.000130	8889.1295	99758	0.000217
8700.9907	96387	0.000326	8860.2193	99240	0.000119	8889.1850	99759	–0.000094
8701.0464	96388	0.000215	8860.2750	99241	0.000008	8889.2412	99760	0.000295
8701.1021	96389	0.000104	8860.3310	99242	0.000197	8889.2968	99761	0.000084
8701.1582	96390	0.000393	8860.3860	99243	–0.000614	8889.3524	99762	–0.000127
8701.2134	96391	–0.000218	8860.4427	99244	0.000275	8889.4085	99763	0.000162
8701.2694	96392	–0.000029	8860.4984	99245	0.000164	8889.4641	99764	–0.000049
8701.3253	96393	0.000060	8860.5545	99246	0.000453	8889.5201	99765	0.000140
8701.3811	96394	0.000049	8860.6099	99247	0.000042	8889.5756	99766	–0.000171
8701.4372	96395	0.000338	8860.6655	99248	–0.000169	8889.6316	99767	0.000018
8701.4928	96396	0.000127	8860.7217	99249	0.000220	8889.6875	99768	0.000107
8701.5490	96397	0.000516	8860.7772	99250	–0.000091	8889.7429	99769	–0.000304
8701.6043	96398	0.000005	8860.8334	99251	0.000298	8889.7993	99770	0.000285
8701.6602	96399	0.000094	8860.8891	99252	0.000187	8889.8547	99771	–0.000126
8701.7161	96400	0.000183	8860.9444	99253	–0.000324	8889.9107	99772	0.000063
8701.7715	96401	–0.000228	8861.0008	99254	0.000265	8889.9666	99773	0.000152
8701.8278	96402	0.000261	8861.0565	99255	0.000154	8890.0220	99774	–0.000259
8701.8835	96403	0.000150	8861.1119	99256	–0.000257	8890.0780	99775	–0.000070
8701.9394	96404	0.000239	8861.1683	99257	0.000332	8890.1337	99776	–0.000181
8701.9952	96405	0.000228	8861.2236	99258	–0.000179	8890.1895	99777	–0.000192
8702.0507	96406	–0.000083	8861.2797	99259	0.000110	8890.2454	99778	–0.000103
8702.1069	96407	0.000306	8861.3356	99260	0.000199	8890.3010	99779	–0.000314
8702.1625	96408	0.000095	8861.3908	99261	–0.000412	8890.3572	99780	0.000075
8702.2185	96409	0.000284	8861.4473	99262	0.000277	8890.4130	99781	0.000064

Table A1—Continued

BJD (2450000+)	*E*	*O*−*C* (day)	*BJD* (2450000+)	*E*	*O*−*C* (day)	*BJD* (2450000+)	*E*	*O*−*C* (day)
8702.2736	96410	–0.000427	8861.5027	99263	–0.000134	8890.4686	99782	–0.000147
8702.3298	96411	–0.000038	8861.5590	99264	0.000355	8890.5248	99783	0.000242
8702.3858	96412	0.000151	8861.6144	99265	–0.000056	8890.5802	99784	–0.000169
8702.4415	96413	0.000040	8861.6699	99266	–0.000367	8890.6363	99785	0.000120
8702.4974	96414	0.000129	8861.7265	99267	0.000422	8890.6921	99786	0.000109
8702.5534	96415	0.000318	8861.7817	99268	–0.000189	8890.7475	99787	–0.000302
8702.6090	96416	0.000107	8861.8379	99269	0.000200	8890.8041	99788	0.000487
8702.6651	96417	0.000396	8861.8934	99270	–0.000111	8890.8593	99789	–0.000124
8702.7207	96418	0.000185	8862.0052	99272	0.000067	8890.9154	99790	0.000165
8702.7766	96419	0.000274	8862.0608	99273	–0.000144	8890.9710	99791	–0.000046
8702.8325	96420	0.000363	8862.1169	99274	0.000145	8891.0268	99792	–0.000057
8702.8879	96421	–0.000048	8862.1728	99275	0.000234	8891.0827	99793	0.000032
8702.9434	96422	–0.000359	8862.2284	99276	0.000023	8891.1384	99794	–0.000079
8702.9997	96423	0.000130	8862.2842	99277	0.000012	8891.1945	99795	0.000210
8703.0557	96424	0.000319	8862.3402	99278	0.000201	8891.2502	99796	0.000099
8703.1114	96425	0.000208	8862.3958	99279	–0.000010	8891.3056	99797	–0.000312
8703.1670	96426	–0.000004	8862.4520	99280	0.000379	8891.3623	99798	0.000577
8703.2229	96427	0.000085	8862.5071	99281	–0.000332	8891.4174	99799	–0.000134
8703.2785	96428	–0.000126	8862.5635	99282	0.000257	8891.5291	99801	–0.000056
8703.3344	96429	–0.000037	8862.6191	99283	0.000046	8891.5847	99802	–0.000267
8703.3897	96430	–0.000548	8862.6747	99284	–0.000165	8891.6409	99803	0.000122
8703.4460	96431	–0.000059	8862.7310	99285	0.000324	8891.6962	99804	–0.000389
8703.5022	96432	0.000330	8862.7865	99286	0.000013	8891.7524	99805	0.000000
8703.5576	96433	–0.000081	8862.8424	99287	0.000102	8891.8081	99806	–0.000111
8703.6134	96434	–0.000092	8862.8980	99288	–0.000109	8891.8636	99807	–0.000422
8703.6697	96435	0.000397	8862.9540	99289	0.000080	8891.9200	99808	0.000167
8703.7250	96436	–0.000114	8863.0100	99290	0.000269	8891.9755	99809	–0.000144
8703.7813	96437	0.000375	8863.0655	99291	–0.000042	8892.0318	99810	0.000345
8703.8368	96438	0.000064	8863.0100	99290	0.000269	8892.0872	99811	–0.000066
8703.8928	96439	0.000253	8863.0655	99291	–0.000042	8892.1425	99812	–0.000577
8703.9487	96440	0.000342	8863.1218	99292	0.000447	8892.1990	99813	0.000112
8704.0041	96441	–0.000069	8863.1769	99293	–0.000264	8892.2541	99814	–0.000599

Table A1—Continued

BJD (2450000+)	*E*	*O*−*C* (day)	*BJD* (2450000+)	*E*	*O*−*C* (day)	*BJD* (2450000+)	*E*	*O*−*C* (day)
8704.0604	96442	0.000420	8863.2330	99294	0.000025	8892.3104	99815	–0.000110
8704.1157	96443	–0.000091	8863.2890	99295	0.000214	8892.3662	99816	–0.000121
8704.1715	96444	–0.000102	8863.3445	99296	–0.000097	8892.4217	99817	–0.000432
8704.2279	96445	0.000487	8863.4008	99297	0.000392	8892.4781	99818	0.000157
8704.2831	96446	–0.000124	8863.4562	99298	–0.000019	8892.5331	99819	–0.000654
8704.3394	96447	0.000365	8863.5120	99299	–0.000030	8892.5895	99820	–0.000065
8704.3952	96448	0.000354	8863.5679	99300	0.000059	8892.6453	99821	–0.000076
8704.4506	96449	–0.000057	8863.6237	99301	0.000048	8892.7009	99822	–0.000287
8704.5069	96450	0.000432	8863.6798	99302	0.000337	8892.7570	99823	0.000002
8704.5622	96451	–0.000079	8863.7351	99303	–0.000174	8892.8122	99824	–0.000609
8704.6182	96452	0.000110	8863.7912	99304	0.000115	8892.8689	99825	0.000280
8704.6741	96453	0.000199	8863.8470	99305	0.000104	8892.9243	99826	–0.000131
8704.7298	96454	0.000088	8863.9027	99306	–0.000007	8892.9800	99827	–0.000242
8704.7855	96455	–0.000023	8863.9588	99307	0.000282	8893.0360	99828	–0.000053
8704.8412	96456	–0.000134	8864.0144	99308	0.000071	8893.0916	99829	–0.000264
8704.8971	96457	–0.000045	8864.0702	99309	0.000060	8893.1478	99830	0.000125
8704.9531	96458	0.000144	8864.1258	99310	–0.000151	8893.2031	99831	–0.000386
8705.0088	96459	0.000033	8864.1814	99311	–0.000362	8893.2590	99832	–0.000297
8705.0647	96460	0.000122	8864.2380	99312	0.000427	8893.3152	99833	0.000092
8705.1202	96461	–0.000189	8864.2934	99313	0.000016	8893.3707	99834	–0.000219
8705.1762	96462	0.000000	8864.3492	99314	0.000005	8893.4267	99835	–0.000030
8705.2320	96463	–0.000011	8864.4051	99315	0.000094	8893.4825	99836	–0.000041
8705.2878	96464	–0.000022	8864.4607	99316	–0.000117	8893.5377	99837	–0.000652
8705.3438	96465	0.000167	8864.5168	99317	0.000172	8893.5940	99838	–0.000163
8705.3993	96466	–0.000144	8864.5724	99318	–0.000039	8893.6496	99839	–0.000374
8705.4552	96467	–0.000055	8864.6283	99319	0.000050	8893.7057	99840	–0.000085
8705.5110	96468	–0.000066	8864.6843	99320	0.000239	8893.7612	99841	–0.000396
8705.5667	96469	–0.000177	8864.7396	99321	–0.000272	8893.8172	99842	–0.000207
8705.6226	96470	–0.000088	8864.7960	99322	0.000317	8893.8733	99843	0.000082
8705.6781	96471	–0.000399	8864.8513	99323	–0.000194	8893.9286	99844	–0.000429
8705.7342	96472	–0.000110	8864.9076	99324	0.000295	8893.9849	99845	0.000060
8705.7902	96473	0.000079	8864.9631	99325	–0.000016	8894.0405	99846	–0.000151

Table A1—Continued

BJD (2450000+)	*E*	*O*−*C* (day)	*BJD* (2450000+)	*E*	*O*−*C* (day)	*BJD* (2450000+)	*E*	*O*−*C* (day)
8705.8459	96474	–0.000032	8865.0188	99326	–0.000127	8894.0961	99847	–0.000363
8705.9017	96475	–0.000043	8865.0751	99327	0.000362	8894.1525	99848	0.000226
8705.9572	96476	–0.000354	8865.1306	99328	0.000051	8894.2079	99849	–0.000185
8706.0130	96477	–0.000365	8865.1864	99329	0.000040	8894.2640	99850	0.000104
8706.0689	96478	–0.000276	8865.2422	99330	0.000029	8894.3194	99851	–0.000307
8706.1250	96479	0.000013	8865.2979	99331	–0.000082	8894.3750	99852	–0.000518
8706.1801	96480	–0.000698	8865.3541	99332	0.000307	8894.4313	99853	–0.000029
8706.2363	96481	–0.000309	8865.4092	99333	–0.000404	8894.4868	99854	–0.000340
8706.2925	96482	0.000080	8865.4654	99334	–0.000015	8894.5431	99855	0.000149
8706.3476	96483	–0.000631	8865.5214	99335	0.000174	8894.5988	99856	0.000038
8706.4041	96484	0.000058	8865.5771	99336	0.000063	8894.6543	99857	–0.000273
8706.4598	96485	–0.000053	8865.6332	99337	0.000352	8894.7106	99858	0.000216
8706.5156	96486	–0.000064	8865.6884	99338	–0.000259	8894.7657	99859	–0.000495
8706.5715	96487	0.000025	8865.7444	99339	–0.000070	8894.8218	99860	–0.000206
8706.6269	96488	–0.000386	8865.8003	99340	0.000019	8894.8780	99861	0.000183
8706.6827	96489	–0.000397	8865.8558	99341	–0.000292	8894.9336	99862	–0.000028
8706.7395	96490	0.000592	8865.9122	99342	0.000297	8894.9894	99863	–0.000039
8706.7949	96491	0.000181	8865.9677	99343	–0.000014	8895.0448	99864	–0.000450
8706.8509	96492	0.000370	8866.0232	99344	–0.000325	8895.1010	99865	–0.000061
8706.9060	96493	–0.000341	8866.0796	99345	0.000264	8895.1565	99866	–0.000372
8706.9622	96494	0.000048	8866.1350	99346	–0.000147	8895.2123	99867	–0.000383
8707.0183	96495	0.000337	8866.1912	99347	0.000242	8895.2686	99868	0.000106
8707.0738	96496	0.000026	8866.2468	99348	0.000031	8895.3239	99869	–0.000405
8707.1297	96497	0.000115	8866.3028	99349	0.000220	8895.3800	99870	–0.000116
8707.1855	96498	0.000104	8866.3585	99350	0.000109	8895.4361	99871	0.000173
8707.2414	96499	0.000193	8866.4141	99351	–0.000102	8895.4914	99872	–0.000338
8707.2972	96500	0.000182	8866.4703	99352	0.000287	8895.5476	99873	0.000051
8707.3526	96501	–0.000229	8866.5259	99353	0.000076	8895.6031	99874	–0.000260
8707.4091	96502	0.000460	8866.5816	99354	–0.000035	8895.6590	99875	–0.000171
8707.4645	96503	0.000049	8866.6377	99355	0.000254	8895.7149	99876	–0.000082
8707.5203	96504	0.000038	8866.6931	99356	–0.000157	8895.7706	99877	–0.000193
8707.5764	96505	0.000327	8866.7493	99357	0.000232	8895.8266	99878	–0.000004

Table A1—Continued

BJD (2450000+)	*E*	*O*−*C* (day)	*BJD* (2450000+)	*E*	*O*−*C* (day)	*BJD* (2450000+)	*E*	*O*−*C* (day)
8707.6317	96506	–0.000184	8866.8050	99358	0.000120	8895.8825	99879	0.000085
8707.6881	96507	0.000405	8866.8606	99359	–0.000091	8895.9381	99880	–0.000126
8707.7437	96508	0.000194	8866.9167	99360	0.000198	8895.9942	99881	0.000163
8707.7994	96509	0.000083	8866.9722	99361	–0.000113	8896.0497	99882	–0.000148
8707.8554	96510	0.000272	8867.0284	99362	0.000276	8896.1057	99883	0.000041
8707.9111	96511	0.000161	8867.0838	99363	–0.000135	8896.1614	99884	–0.000070
8707.9670	96512	0.000250	8867.1400	99364	0.000254	8896.2172	99885	–0.000081
8708.0227	96513	0.000139	8867.1957	99365	0.000143	8896.2732	99886	0.000108
8708.0786	96514	0.000228	8867.2514	99366	0.000032	8896.3285	99887	–0.000403
8708.1347	96515	0.000517	8867.3074	99367	0.000221	8896.3850	99888	0.000286
8708.1897	96516	–0.000294	8867.3631	99368	0.000110	8896.4405	99889	–0.000025
8708.2462	96517	0.000395	8867.4189	99369	0.000099	8896.4963	99890	–0.000036
8708.3020	96518	0.000384	8867.4749	99370	0.000288	8896.5522	99891	0.000053
8708.3574	96519	–0.000027	8867.5304	99371	–0.000023	8896.6080	99892	0.000042
8708.4133	96520	0.000062	8867.5866	99372	0.000366	8896.6640	99893	0.000231
8708.4687	96521	–0.000349	8867.6424	99373	0.000355	8896.7192	99894	–0.000380
8708.5249	96522	0.000040	8867.6981	99374	0.000244	8896.7752	99895	–0.000191
8708.5807	96523	0.000029	8867.7538	99375	0.000133	8896.8311	99896	–0.000102
8708.6364	96524	–0.000082	8867.8095	99376	0.000022	8896.8870	99897	–0.000013
8708.6925	96525	0.000207	8867.8657	99377	0.000411	8896.9429	99898	0.000076
8708.7478	96526	–0.000304	8867.9209	99378	–0.000200	8896.9984	99899	–0.000235
8708.8039	96527	–0.000015	8867.9772	99379	0.000289	8897.0547	99900	0.000254
8708.8598	96528	0.000074	8868.0329	99380	0.000178	8897.1101	99901	–0.000157
8708.9157	96529	0.000163	8868.0886	99381	0.000067	8897.1659	99902	–0.000168
8708.9715	96530	0.000152	8868.1449	99382	0.000556	8897.2222	99903	0.000321
8709.0268	96531	–0.000359	8868.1997	99383	–0.000455	8897.2779	99904	0.000210
8709.0831	96532	0.000130	8868.2560	99384	0.000034	8897.3334	99905	–0.000101
8709.1389	96533	0.000119	8868.3120	99385	0.000223	8897.3892	99906	–0.000112
8709.1944	96534	–0.000192	8868.3674	99386	–0.000188	8897.4451	99907	–0.000023
8709.2508	96535	0.000397	8868.4235	99387	0.000101	8897.5011	99908	0.000166
8709.3060	96536	–0.000214	8868.4785	99388	–0.000710	8897.5566	99909	–0.000145
8709.3619	96537	–0.000125	8868.5352	99389	0.000179	8897.6125	99910	–0.000056

Table A1—Continued

BJD (2450000+)	*E*	*O*−*C* (day)	*BJD* (2450000+)	*E*	*O*−*C* (day)	*BJD* (2450000+)	*E*	*O*−*C* (day)
8709.4174	96538	–0.000436	8868.5912	99390	0.000368	8897.6685	99911	0.000133
8709.4737	96539	0.000053	8868.6466	99391	–0.000043	8897.7240	99912	–0.000178
8709.5298	96540	0.000342	8868.7028	99392	0.000346			
8709.5850	96541	–0.000269	8868.7581	99393	–0.000165			

Note. — T_{max} is the observed times of maximum light of GSC 4552-1498. E: Cycle number. $O-C$ is in days. E and $O-C$ are based on the ephemris formula: $BJD_{max} = T_0 + P \times E = 2453321.534728(1) + 0.055811(0) \times E$.

Table A2. 79 Previous Times of Maximum Light and $O-C$ Values of GSC 4552-1498.

BJD (2450000+)	*E*	$O-C$ (day)	*S*	*BJD* (2450000+)	*E*	$O-C$ (day)	*S*
3321.5361	0	0.001372	1	6001.4116	48017	–0.000308	3
3321.5919	1	0.001361	1	6001.4673	48018	–0.000419	3
3321.6481	2	0.001750	1	6001.5230	48019	–0.000530	3
3321.7032	3	0.001039	1	6001.5791	48020	–0.000241	3
3534.3990	3814	0.001087	1	6001.6346	48021	–0.000552	3
3534.4550	3815	0.001276	1	6002.3041	48033	–0.000784	3
3792.3016	8435	0.001018	1	6002.3596	48034	–0.001095	3
3792.3574	8436	0.001007	1	6002.4158	48035	–0.000706	3
3810.3281	8758	0.000562	1	6064.4780	49147	–0.000347	3
3810.3840	8759	0.000651	1	6064.5336	49148	–0.000558	3
3810.4396	8760	0.000440	1	6075.5289	49345	–0.000027	3
4172.3742	15245	0.000652	1	6075.5839	49346	–0.000838	3
4172.4298	15246	0.000441	1	6305.6930	53469	–0.000525	4
4172.4863	15247	0.001130	1	6336.5007	54021	–0.000501	4
4172.5415	15248	0.000519	1	6356.5925	54381	–0.000664	4
4172.5973	15249	0.000508	1	6356.6484	54382	–0.000575	4
4172.6529	15250	0.000297	1	6385.5028	54899	–0.000467	4
4209.3211	15907	0.000665	1	6385.5584	54900	–0.000678	4
4209.3772	15908	0.000954	1	6506.4457	57066	–0.000021	4
5580.4286	40474	–0.000873	2	6692.6865	60403	–0.000556	5
5580.4846	40475	–0.000684	2	6692.7427	60404	–0.000167	5
5580.5402	40476	–0.000895	2	6698.3790	60505	–0.000778	6
5580.5960	40477	–0.000906	2	6698.4352	60506	–0.000389	6
5580.6520	40478	–0.000718	2	6698.4911	60507	–0.000300	6
5640.3697	41548	–0.000796	2	6698.5473	60508	0.000089	6
5640.3701	41548	–0.000396	2	6725.3359	60988	–0.000595	5
5640.4259	41549	–0.000407	2	6725.3917	60989	–0.000606	5
5646.2858	41654	–0.000663	2	6725.4473	60990	–0.000817	5
5646.3415	41655	–0.000774	2	6741.3542	61275	–0.000055	5
5646.3975	41656	–0.000585	2	6741.4098	61276	–0.000266	5
5646.4531	41657	–0.000796	2	6741.4660	61277	0.000123	5
5683.4007	42319	–0.000084	2	6749.6131	61423	–0.001184	5

Table A2—Continued

BJD (2450000+)	*E*	*O*−*C* (day)	*S*	*BJD* (2450000+)	*E*	*O*−*C* (day)	*S*
5941.4142	46942	–0.000874	3	6749.6692	61424	–0.000895	5
5941.4702	46943	–0.000685	3	6757.4269	61563	–0.000925	5
5941.5257	46944	–0.000996	3	6903.4290	64179	–0.000423	5
5962.2876	47316	–0.000791	3	6958.6254	65168	–0.001110	5
5962.3433	47317	–0.000902	3	6958.6818	65169	–0.000521	5
5962.3992	47318	–0.000813	3	6968.2812	65341	–0.000614	5
6001.3001	48015	–0.000186	3	6968.3370	65342	–0.000625	5
6001.3554	48016	–0.000697	3				

Note. — T_{max} is the observed times of maximum light in BJD - 2450000. E: Cycle number. $O-C$ is in days. E and $O-C$ are based on the ephemris formula: $BJD_{max} = T_0 + P \times E = 2453321.534728(1) + 0.055811(0) \times E$. Source: (1) Wils et al. 2009; (2) Wils et al. 2012; (3) Wils et al. 2013; (4) Wils et al. 2014; (5) Wils et al. 2015; (6) Jafarzadeh & Poro 2017.